Coastal Engineering xxx (2011) xxx–xxx

Contents lists available at ScienceDirect

Coastal Engineering

journal homepage: www.elsevier.com/locate/coastaleng

A heuristic examination of cohesive sediment bed exchange in turbulent flows

J.V. Letter, Jr. [a], A.J. Mehta [b,*]

[a] Coastal and Hydraulics Laboratory, U.S. Army Engineer Research and Development Center, Vicksburg, MS 39180, USA
[b] Department of Civil and Coastal Engineering, University of Florida, Gainesville, FL 32611, USA

ARTICLE INFO

Article history:
Received 30 June 2010
Received in revised form 30 March 2011
Accepted 11 April 2011
Available online xxxx

Keywords:
Deposition
Erosion
Floc shear strength
Marine environment
Probabilistic variables
Suspended sediment concentration

ABSTRACT

Prediction of the concentration of suspended cohesive sediment in the marine environment is constrained by difficulties in interpreting experimental evidence on bed exchange, i.e. erosion and deposition of particles, which remains sparse in mechanistic details. In this paper, conditions under which bed exchange in turbulent flows collectively determines the concentration of suspended matter have been examined in the heuristic sense based on selective experimental data. It is argued that interpretation of such data can be significantly facilitated when multi-class representation of particle size, collisional interaction between suspended particles and probabilistic representations of the bed shear stress along with variables describing particle behavior (critical shear stress for deposition, bed floc shear strength) are taken into account. Aggregation—floc growth and breakup kinetics—brings about shifts in the suspended particle size distribution; bed exchange is accordingly modulated and this in turn determines concentration dynamics. Probabilistic representation of the governing variables broadens the suspended sediment size spectrum by increasing the possibilities of inter-particle interactions relative to the mean-value representation. Simple models of bed exchange, which essentially rely on single-size assumption and mean-value representation of variables, overlook the mechanistic basis underpinning particle dynamics.

1. Introduction

Erosion of cohesive sediment in turbulent boundary layer flows is often modeled using expressions for the sediment flux driven by the bed shear stress as a mean-value variable, and disregarding ubiquitous heterogeneity in particle size. To obviate this hurdle, present-day numerical modeling approaches using multi-phase equations for flow and sediment transport internalize the bed-water boundary and thereby attempt to bypass the use of expressions for sediment fluxes at the bed (e.g. Hsu et al. 2007). However, in numerous instances of engineering and ecohydrological interest such a "continuous-phase" modeling protocol is tedious, and explains the continued popularity of models based on the mean-value approach (Wolanski 2007).

Unfortunately, the simple approach raises questions regarding the validity of assumptions that are invoked when deposition is modeled in combination with erosion. In this paper we evaluate some of these constraining assumptions of the simple mean-valued approach. We will attempt to elaborate on the underpinning limitations based on a heuristic interpretation of previous experimental data on cohesive sediment bed exchange, i.e. erosion and deposition. The significance of coupling multi-class representation of sediment size and probabilistic variables governing bed exchange is examined using the numerical laboratory approach (e.g. Tolhurst et al. 2009), which incorporates the effects of aggregation, i.e. the kinetics of floc growth and breakup, on eroding and depositing sediment. An analytical strength of numerical experiments is that they permit the determination of net bed exchange from gross erosion and deposition fluxes, which are typically not measured separately in laboratory experiments.

2. Physical basis

Cohesive sediment characteristically conforms to a different transport regime than cohesionless particles. In the probabilistic development of Einstein (1950) for the transport of sand, the condition of equality between eroding and depositing particle number fluxes is postulated. In order to interpret this development in terms of the transport of flocculated cohesive sediment, Partheniades (1965) considered all flocs to be effectively identical with a uniform shear strength τ_s (equivalent to the critical shear stress for erosion τ_{cr} of cohesionless sediment) resisting erosion. As a consequence, for treatment of flocs of different sizes the Partheniades model must be applied repeatedly to each size as in the development of Einstein for sand, and the total erosion flux calculated as the sum of contributions from all size classes. This essentially means that aggregation involving interactions between suspended particles of different sizes is ignored. Therefore, that approach cannot account for experimentally observed shifts in the size distribution of suspended flocs arising mainly from aggregation due to turbulent shear, and to a lesser extent due to differential settling and Brownian motion (Winterwerp and van Kesteren 2004). Another ramification of the single-size assumption is

* Corresponding author. Tel.: +1 352 3929537.
E-mail address: mehta@coastal.ufl.edu (A.J. Mehta).

0378-3839/$ – see front matter © 2011 Elsevier B.V. All rights reserved.
doi:10.1016/j.coastaleng.2011.04.003

Report Documentation Page

Form Approved
OMB No. 0704-0188

1. REPORT DATE	2. REPORT TYPE	3. DATES COVERED
2011		**00-00-2011 to 00-00-2011**

4. TITLE AND SUBTITLE	5a. CONTRACT NUMBER
A Heuristic Examination Of Cohesive Sediment Bed Exchange In Turbulent Flows	5b. GRANT NUMBER
	5c. PROGRAM ELEMENT NUMBER
6. AUTHOR(S)	5d. PROJECT NUMBER
	5e. TASK NUMBER
	5f. WORK UNIT NUMBER
7. PERFORMING ORGANIZATION NAME(S) AND ADDRESS(ES) **U.S. Army Engineer Research and Development Center,Coastal and Hydraulics Laboratory,Vicksburg,MS,39180**	8. PERFORMING ORGANIZATION REPORT NUMBER
9. SPONSORING/MONITORING AGENCY NAME(S) AND ADDRESS(ES)	10. SPONSOR/MONITOR'S ACRONYM(S)
	11. SPONSOR/MONITOR'S REPORT NUMBER(S)

12. DISTRIBUTION/AVAILABILITY STATEMENT
Approved for public release; distribution unlimited

13. SUPPLEMENTARY NOTES
In Coastal Engineering Article in Press, Corrected Proof,2011

14. ABSTRACT
Prediction of the concentration of suspended cohesive sediment in the marine environment is constrained by difficulties in interpreting experimental evidence on bed exchange, i.e. erosion and deposition of particles,which remains sparse in mechanistic details. In this paper, conditions under which bed exchange in turbulent flows collectively determines the concentration of suspended matter have been examined in the heuristic sense based on selective experimental data. It is argued that interpretation of such data can be significantly facilitated when multi-class representation of particle size, collisional interaction between suspended particles and probabilistic representations of the bed shear stress along with variables describing particle behavior (critical shear stress for deposition, bed floc shear strength) are taken into account. Aggregation? floc growth and breakup kinetics?brings about shifts in the suspended particle size distribution; bed exchange is accordingly modulated and this in turn determines concentration dynamics. Probabilistic representation of the governing variables broadens the suspended sediment size spectrum by increasing the possibilities of inter-particle interactions relative to the mean-value representation. Simple models of bed exchange, which essentially rely on single-size assumption and mean-value representation of variables,overlook the mechanistic basis underpinning particle dynamics.

15. SUBJECT TERMS

16. SECURITY CLASSIFICATION OF:			17. LIMITATION OF ABSTRACT	18. NUMBER OF PAGES	19a. NAME OF RESPONSIBLE PERSON
a. REPORT **unclassified**	b. ABSTRACT **unclassified**	c. THIS PAGE **unclassified**	**Same as Report (SAR)**	**12**	

that even though the bed shear stress τ_b represented by its probability density function (pdf) is time-dependent, at any instant only erosion can occur if τ_b is greater than τ_s and only deposition when τ_b is lower than τ_s. Observe that a change in the floc size distribution of suspended sediment can occur through exchange of flocs with the bed deposit. However, to reproduce the loss of the finest flocs in a flow condition that excludes deposition of those flocs requires the inclusion of aggregation processes in the analysis.

For tidal flows the pictorial depiction in Fig. 1a of the exclusive erosion or deposition paradigm requires a sub-division of the flood and the ebb phases of the tidal cycle into sub-periods. Starting from slack water the first sub-period, in which only deposition (flux δ) can occur, corresponds to the duration when the bed shear stress τ_b is less than the critical shear stress for deposition τ_d, i.e. the stress below which all initially suspended (single-size) sediment deposits and above which remains in suspension indefinitely (Krone 1962). In the second sub-period τ_b is between τ_d and the bed floc shear strength τ_s, which must be exceeded by τ_b for erosion to occur. In this sub-period there is neither erosion (flux ε) nor deposition. In the third sub-period, when τ_b is greater than τ_s, there can be erosion but no deposition. The reverse sequence follows as the bed shear stress begins to decrease past its peak value at the strength of flow.

Physical evidence supporting the sequence of processes in Fig. 1a has not been found in the marine environment. Sanford and Halka (1993) used a numerical modeling approach based on single size to explain the transport of tidally suspended fine sediment in the Chesapeake Bay. They showed that in order to reproduce the measured concentration time-series in the bay it was essential to permit continuous deposition (Fig. 1b); when the exclusive paradigm was used predictions were unsatisfactory. An important feature of this finding is that when the flow velocity is sufficiently high, there can be a sub-period when erosion and deposition occur simultaneously. An equally important inference, further elaborated upon by van Prooijen and Winterwerp (2010), is that in order to implement the single-size model in conjunction with continuous deposition, in addition to the bed shear stress the floc shear strength must be treated as a probabilistic variable. This is so because an overlap in the tails of the pdfs of these two variables is essential for simultaneous erosion and deposition to occur at the bed surface. By including the shear strength as a spatially distributed variable, the instantaneous bed shear stress will always be less than the shear strength somewhere, and make deposition possible. In addition, variability of the floc shear strength for a given size class is influenced by the inherent non-uniformity in the size of the primary particles from which the flocs are formed. This also affects the variability in the floc density and fall velocity for flocs within that size class. As we will see an extension of the Sanford and Halka model to account for multiple size classes and incorporating the probabilistic approach has important consequences with regard to the prediction of time-varying suspended sediment concentration.

3. Experimental data

The experiments selected to explore the exclusive and continuous-deposition paradigms include tests previously carried out in a counter-rotating annular flume (CRAF). This apparatus consisted of a 0.2 m wide and 0.45 m deep annular channel with a mean diameter of 1.5 m. Water in the channel was driven by shear generated from a rotating upper lid, with the ability to rotate the channel in the opposite direction from the ring to minimize radial secondary currents.

In a series of deposition-dominated tests, a kaolinite clay flocculated with small quantities of salt in 0.31 m deep water was used (Mehta 1973). In each test run the sediment was initially suspended at a concentration of 1 kg m^{-3} and then permitted to

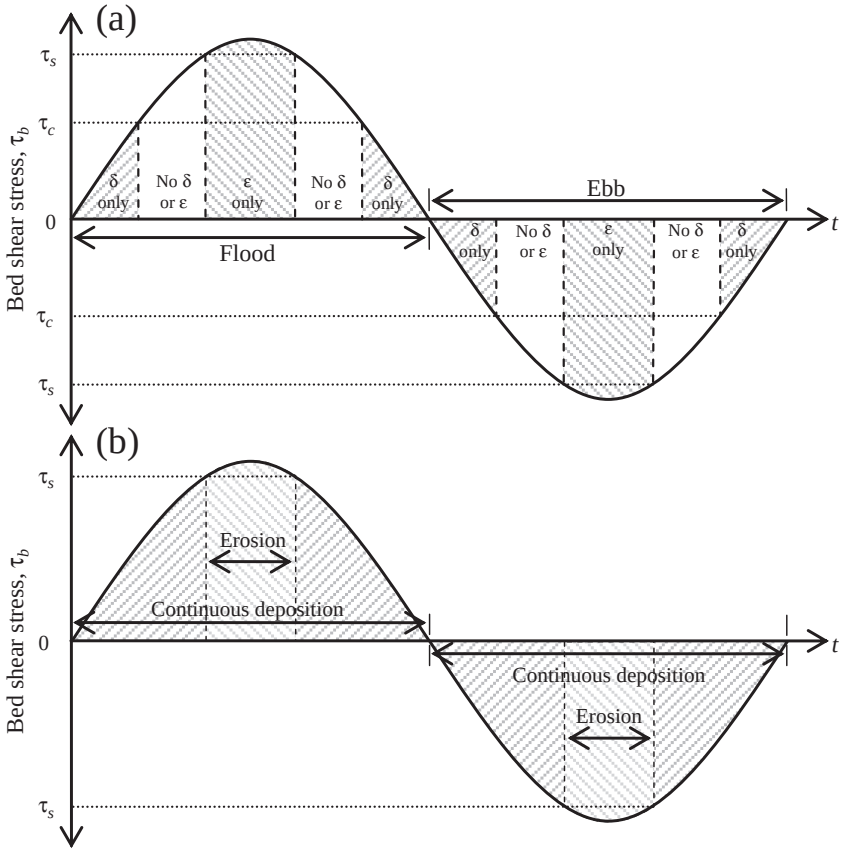

Fig. 1. Sub-periods of deposition flux (δ), erosion flux (ε) and no bed exchange during a tidal cycle: (a) Exclusive paradigm; (b) continuous-deposition paradigm.

Please cite this article as: Letter, J.V., Mehta, A.J., A heuristic examination of cohesive sediment bed exchange in turbulent flows, Coast. Eng. (2011), doi:10.1016/j.coastaleng.2011.04.003

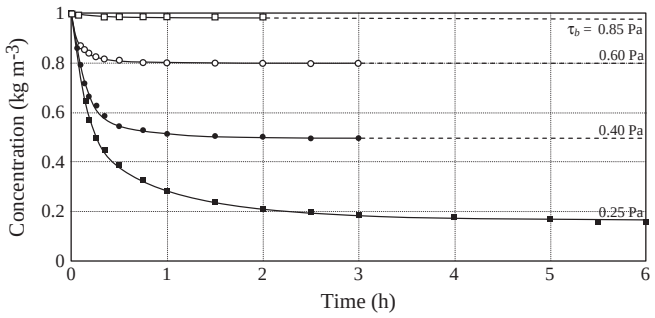

Fig. 2. Time-variation of depth-mean suspended sediment concentration of kaolinite in CRAF tests of Mehta (1973) at four bed shear stresses. Curves are mean trends and dashed lines are extrapolated trends.

deposit at a constant bed shear stress. The depth–mean suspended sediment concentration was recorded at different times. Data points and mean trends from four runs, in which the shear stresses were 0.25, 0.40, 0.60 and 0.85 Pa, are plotted in Fig. 2. In each case the concentration fell and approached a residual value which increased with the bed shear stress. Mehta and Partheniades (1975) attempted to explain this behavior under the assumption that even though aggregation likely occurred, the overall size distribution of the mixture of flocs and any non-flocculated large particles remained unaffected during deposition. From this assumption, which considers that there is little *net* effect of aggregation on the size distribution, it follows that once the concentration becomes practically constant there was no further deposition or erosion. The remaining suspension merely consisted of particles that were small or weakly flocculated and stayed on the bed only for very short residence times. Thus it was inferred that the residual concentration is effectively a steady-state value with practically zero erosion and deposition fluxes, rather than the outcome of equilibrium between the two fluxes. Since during deposition floc size distributions were not measured in the study, this inference could not be verified.

In a separate experiment in the CRAF, a bed of flocculated kaolinite from the same source as in the deposition runs was eroded for a period of 120 h in water depth of 0.26 m at a bed shear stress of 0.20 Pa (Parchure 1984, Parchure and Mehta 1985). The erosion flux steadily decreased and the suspended sediment concentration, which was reasonably uniform over depth, approached 3.85 kg m^{-3} in about an hour and remained practically unchanged during the remainder of the test (Fig. 3). After 120 h the entire volume of suspension was replaced over a period of 4 h with sediment-free water introduced at a constant rate (8.77×10^{-5} $m^3 s^{-1} m^2$), without disturbing the bed or changing the flow velocity. At the end of the 4-hour period, concentration in the channel had decreased to 0.030 kg m^{-3}. The flow was maintained for an additional 24 h during which the concentration increased to 0.1 kg m^{-3}.

4. Multi-class representation

For an assessment of bed exchange with reference to the above tests, we will rely in part on two experimental relationships among the governing variables, one for settling particles and the other for particles at the bed surface. Since these relationships are deduced from different investigations they are postulated to be representative of qualitative trends inherent to the transport of kaolinite flocs in the CRAF.

For simplicity of treatment and because flocculation of kaolinite flocs can vary depending on the primary particle size and stress history, let d_i represent the diameter of a particle of class-*i* without reference to its exact state of flocculation. When flocs grow by aggregation, they tend to have an increasingly open structure which means that their density decreases (Khelifa and Hill 2006). Thus, although the settling velocity increases with diameter, the rate of increase is lower than it would be if the density remained invariant.

Mehta and Lott (1987) showed that a mean-value relationship exists between the critical shear stress for deposition τ_{di} and the floc settling velocity, consistent with the test runs of Fig. 2. This relationship can be interpreted with respect to diameter d_i of the falling flocs as

$$\tau_{di} = \tau_{d1}\left(\frac{d_i}{d_1}\right)^{\xi} \tag{1}$$

where τ_{d1} is the value of τ_{di} associated with the smallest diameter d_1 and the exponent ξ depends on sediment composition. At a relatively low shear stress turbulence can keep only very small particles in suspension. Larger particles may have sufficient mass and fall velocity to overcome turbulence to reach the bed. As the shear stress increases, the threshold size between entrainment and deposition also increases. For a fixed size at stresses below τ_{di} the particle can overcome entrainment, and above τ_{di} turbulence will keep the particle in suspension.

For a given τ_b the total deposition flux is the sum of the fluxes for each size class, and for each class it is the product of the class settling velocity, suspended sediment concentration and a probability of re-entrainment of the particle about to settle. This probability varies with τ_b; it is zero when $\tau_b = 0$ (i.e. all falling particles of the class remain on the bed). When $\tau_b = \tau_{di}$ the probability is 1, which means that at this (and greater) shear stresses no particles of the class can deposit; all are re-entrained once they are close to the bed where the flow shear rate is the highest in the water column (Krone 1962, Mehta and Partheniades 1975).

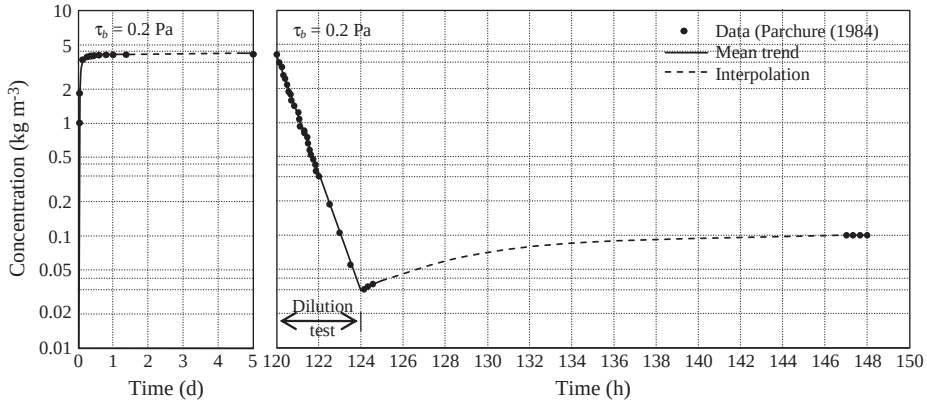

Fig. 3. Erosion and dilution test of Parchure (1984) using kaolinite in the CRAF.

Please cite this article as: Letter, J.V., Mehta, A.J., A heuristic examination of cohesive sediment bed exchange in turbulent flows, Coast. Eng. (2011), doi:10.1016/j.coastaleng.2011.04.003

In regard to flocs on the bed, based on the interpretation made by McAnally and Mehta (2001), the class shear strength τ_{si} can be shown to be related to diameter d_i by the relationships

$$\tau_{si} = 0.256 A_s \left(\frac{\Delta\rho_s}{\rho_w}\right)^{2/(3-D_f)} \left(\frac{d_1}{d_i}\right)^2; \quad \tau_{si} > 0.326 \text{ Pa}$$
$$\tau_{si} = 0.289 \sqrt{A_s \left(\frac{\Delta\rho_s}{\rho_w}\right)^{2/(3-D_f)} \left(\frac{d_1}{d_i}\right)^2}; \quad \tau_{si} \le 0.326 \text{ Pa} \tag{2}$$

where ρ_w is nominally the density of water and the coefficient A_s varies with sediment composition. These relationships are piecewise approximations of a single experimental curve derived from the viscometric tests of Migniot (1968) and Krone (1963) on a variety of fine sediments, and representation of flocs as fractals of dimension D_f according to Kranenburg (1994). Eq. (2) represents a reduction, with increasing floc size, of the resistance of the bonds within the floc to breakage and separation from the bed. In contrast, the trend of increasing critical shear stress for deposition with floc size in Eq. (1) is a measure of the hydrodynamic influence on the floc. Once a floc deposits its size identity is lost over time, as its structure is altered by bed shear, consolidation and gelation. The need to recognize this difference between a depositing and an eroding floc was pointed out by Krone (1963) and later by Winterwerp and van Kesteren (2004).

A qualitative interpretation of Eqs. (1) and (2) has been made in Fig. 4 showing the variation with diameter d of the critical shear stress for deposition τ_d and the bed shear strength τ_s. The subscript i is dropped for convenience, and d represents particles in suspension relative to Eq. (1) and on the bed relative to Eq. (2). Starting with the smallest diameter d_1, the $\tau_d(d)$ curve of Eq. (1) ends at $d = d_*$ where it meets the $\tau_s(d)$ curve from Eq. (2). Define the shear stress at that *junction* as $\tau_d^* = \tau_s(d_*) = \tau_d(d_*)$. In the range of diameters $d > d_*$, the $\tau_d(d)$curve is constrained to follow the $\tau_s(d)$curve, which continues to fall as the flocs become larger and weaker. In other words, for $d > d^*$, $\tau_d(d) = \tau_s(d)$, and the shear strength τ_s is the sole erosion and deposition threshold parameter, i.e. there is erosion when $\tau_b > \tau_s$, while deposition occurs when $\tau_b < \tau_s$. When $\tau_b > \tau_d^*$ there is no deposition of any *cohesive* size class irrespectively of the magnitude of τ_b.

Another interpretation of Fig. 4 can be made by conveniently letting d_i represent the primary particle diameter at the bed surface. As this diameter increases the particle's specific surface area decreases, and the particle's ability to cohere also decreases. With increasing size the $\tau_s(d)$ curve can be expected to approach the trend of the critical shear stress for erosion τ_{cr} of non-cohesive particles.

The diameter d^* depends on the mineral content, particle size distribution, shape and surface texture. Its value appears to be on the order of 10 μm in terms of primary size (Bagnold 1966, Mehta and Lee, 1994). In Fig. 4, as the slope of the $\tau_s(d)$curve decreases, and cohesion effectively vanishes; the $\tau_s(d) = \tau_{cr}(d)$curve levels off before rising at larger diameters. There is some evidence to support this description; the experimental results of Mantz (1977) on the critical shear stress for the erosion of mica flakes, which are fine-grained but largely non-cohesive, yielded a minimum value of $\tau_{cr} = 0.35$ Pa at $d = 23.5$ μm, with larger critical stresses for both lower and higher diameters.

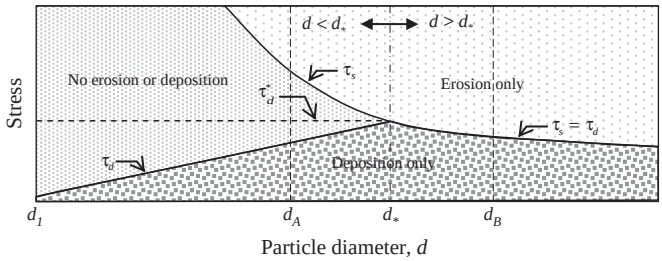

Fig. 4. Zones of bed exchange defined by (mean-value) relationships between the critical shear stress for deposition, shear strength and particle diameter.

In Fig. 4 consider a diameter $d_A < d^*$. Depending on the instantaneous value of bed shear stress τ_b, there can be only deposition when $\tau_b < \tau_d$, neither deposition nor erosion when $\tau_b < \tau_d < \tau_s$, and only erosion when $\tau_b > \tau_s$. For diameter $d_B > d^*$ there can be only erosion ($\tau_b > \tau_s$), or only deposition ($\tau_b < \tau_s$). At diameter d_B no shear stress zone exists in which erosion and deposition can be absent simultaneously, as would occur in the single-size model. In fact the general applicability of the single-size model is severely restrictive because floc diameter, density and shear strength are almost always distributed. As a consequence, at a given bed shear stress, while flocs of size d_A might be depositing, flocs of size d_B could be eroding. Including the effects of density and shear strength complicates transport by adding more scenarios of bed exchange.

In reference to Fig. 4, with the classical mean-valued approach the very finest material can only deposit at very low shear stresses. In the marine environment the duration of these shear stresses may not permit significant deposition due to the low settling velocities. Consequently, a primary mechanism for reduction of concentrations of the finest particles is by flocculation forming larger flocs that then may deposit at higher shear stress levels. This tendency remains with the probabilistic treatment; however, the chances of fine sediment deposition can be increased with the probabilistic treatment of the variables, including the settling velocity. With use of the continuous-deposition assumption, the finest sediments can overcome the tendency to be immediately re-entrained.

Another restriction on the fixed single-size approach is that in estuaries aggregation tends to change the size, density and shear strength distributions of suspended particles during the tidal cycle, which cannot be modeled using that approach. Winterwerp (1998) dealt with this issue by proposing a single representative particle size model that varies the floc size with the level of turbulence. Key features of settling column tests could be replicated using forced shear. It was also found that the residence time plays an important role in the attainment of near-equilibrium floc size with the level of turbulence.

The bed exchange zones proposed in Fig. 4 can be assessed with reference to the deposition-dominated data from Fig. 2. To that end the effect of changing the bed shear stress τ_b between the low experimental value of 0.25 Pa and high 0.85 Pa on bed exchange is illustrated in Fig. 5 for the model of Fig. 4. Typical coefficient values in Eqs. (1) and (2) relevant to the transport of kaolinitic sediment are given in Table 1. The selected range of particle diameters is 0.1 to 1000 μm, although no particular treatment is included to separate well-formed flocs from other particles. The diameter 0.1 μm is consistent with the smallest measured primary particle diameter in the experiments, whereas 1000 μm represents a large macrofloc. A noteworthy observation is that while the data points in Fig. 2 corresponding to the two bed shear stresses indicate net deposition, the conceptual model includes active zones of erosion. At $\tau_b = 0.25$ Pa, deposition occurs over a size range of approximately 1.5 to 15 μm, whereas above 15 μm erosion takes place. Below 1.5 μm particles will neither deposit nor erode when the shear stress is 0.25 Pa. As τ_b is increased the deposition zone decreases rapidly because the zone of erosion extends to smaller sizes and the zone of no erosion or deposition extends to larger particle sizes. At 0.85 Pa, just below τ_d^*, deposition occurs only in the proximity of $d_* = 8$ μm. However, erosion is prevalent over a size range larger than just above d_*, and the zone of no deposition or erosion extends to just smaller than d_*. Above a bed shear stress τ_d^* of 1 Pa no deposition can occur. In general, variability in particle size permits identification of the domains of erosion and deposition implying simultaneous exchange not evident in Fig. 2. Also identified by shading in Fig. 5 is the zone for each shear stress in which there is neither erosion nor deposition within which any particles present in water will remain suspended. For the 0.25 Pa

Please cite this article as: Letter, J.V., Mehta, A.J., A heuristic examination of cohesive sediment bed exchange in turbulent flows, Coast. Eng. (2011), doi:10.1016/j.coastaleng.2011.04.003

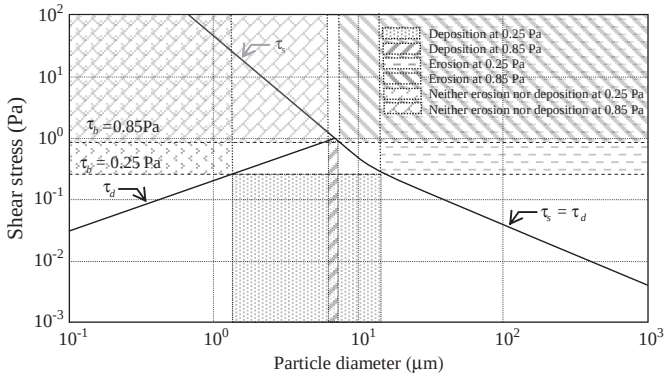

Fig. 5. Zones of bed exchange defined by (mean-value) relationships between the critical shear stress for deposition, shear strength and particle diameter. The plot is based on deposition-dominated data shown in Fig. 2.

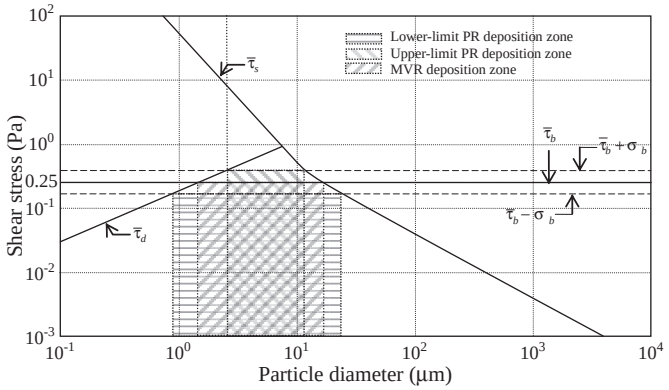

Fig. 6. Zones of bed exchange defined by (mean-value) relationships between the critical shear stress for deposition, shear strength and particle diameter. Unlike Fig. 5, the shear stress is represented probabilistically.

shear stress that zone is below 1.5 μm, and for the 0.85 Pa shear stress is below 7 μm. Note that while Fig. 5 identifies bed exchange zones, it does not define the magnitudes of erosion and deposition fluxes controlling the rate of change of suspended sediment concentration.

5. Effects of probabilistic variables

Based on their modeling and field experimental effort, Sanford and Halka (1993) proposed that when using a single constant particle size, agreement with field observations of suspended concentration would be improved if the governing variables are represented by their pdfs, resulting in sub-periods of simultaneous bed exchange during a tidal cycle in Fig. 1b. This would be the case because in that circumstance at any instant there can be erosion somewhere on the bed and deposition at some other sites. In order to examine the significance of the governing variables on realistic modes of bed exchange we will adopt probabilistic representations for the bed shear stress $\tau_b(t)$, the critical shear stress for deposition τ_{di} and the shear strength τ_{si} in the multi-size model.

The variables τ_b, τ_{di} and τ_{si} are resolved into their mean values and fluctuations, i.e. $\tau_b(t) = \overline{\tau}_b + \tau'_b(t)$, $\tau_{di}(A) = \overline{\tau}_{di} + \tau'_{di}(A)$, and $\tau_{si}(A) = \overline{\tau}_{si} + \tau'_{si}(A)$, respectively, where t denotes time and A signifies variation over the bed surface area. The fluctuations in τ_{di} and τ_{si} can also be associated with non-uniformity in the floc structure within the specified size class. The standard deviations of the respective pdfs are σ_b, σ_{di} and σ_{si}. A probabilistic representation of only the bed shear stress in Fig. 6 illustrates the effects of such a treatment on the bed exchange zones. The critical shear stress for deposition and particle shear strength are illustrated as mean values at each particle size for illustration of the effects of just the probabilistic shear stress. Unlike the distinct boundaries of bed exchange zones in Fig. 5, probabilistic representation of the shear stress introduces variability in the boundaries of these zones. For illustrative purposes τ_b is assumed to be normally distributed, and the respective bands represent ± 1 standard deviation relative to the mean.

Table 1
Deposition and deposition parameters for kaolinite. Source: Letter (2009).

τ_{c1} (Pa)	0.03
d_{f1} (μm)	0.1
ξ_e	0.8
$\Delta\rho_s$ (kg m^{-3})	1650
ρ_w (kg m^{-3})	1000
A_s	1800
D_f	2.2

Probabilistic representation (PR) of τ_b, whose mean value is taken as 0.25 Pa, has qualitatively the same effect as when the mean value is changed, e.g. between 0.25 Pa and 0.85 Pa, in the mean-value representation (MVR) of Fig. 5. Thus while the MVR bed exchange zones remain fixed, fluctuations induce variability in each zone between a lower- and an upper-limit value. Since the size range of particles acted on by the shear stress changes from instant to instant, both erosion and deposition can occur simultaneously even though the critical shear stress for deposition and shear strength are mean-valued. If the full range of the pdfs were considered rather than just ± 1 standard deviation, the effects of variability in τ_b would be even more pronounced.

In the more complex but realistic depiction in Fig. 7, all three governing variables are represented by their distributions. The critical shear stress for deposition τ_d and the shear strength τ_s introduce variability in values defining their respective boundaries. The band for each variable illustrated covers ± 1 standard deviation relative to the mean assuming normally distributed pdfs. While the MVR deposition zone remains fixed as before, the lower-limit of the PR deposition zone is the intersection of the $\overline{\tau}_b - \sigma_b$ boundary with the $\overline{\tau}_d + \sigma_d$ boundary and the upper-limit the intersection of the $\overline{\tau}_b - \sigma_b$ boundary with the $\overline{\tau}_s + \sigma_s$ boundary. The zone of no deposition or erosion (not shaded in Fig. 7) becomes much smaller due to the probabilistic treatment of both the shear stress and the critical shear stress for deposition. For a broader range of probabilities (e.g., ± 2 or 3 standard deviations) the zones of no deposition or erosion would become very small, at only the smallest particle sizes. The effect of variance in each

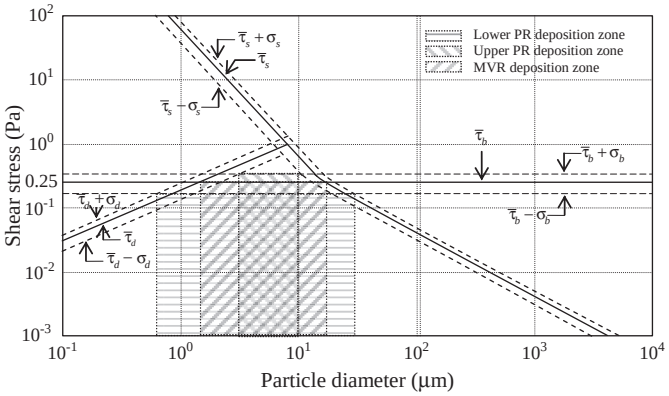

Fig. 7. Zones of bed exchange defined by relationships between the critical shear stress for deposition, the shear strength and particle diameter. Unlike Fig. 6, the critical shear stress for deposition and the shear strength are represented probabilistically.

Please cite this article as: Letter, J.V., Mehta, A.J., A heuristic examination of cohesive sediment bed exchange in turbulent flows, Coast. Eng. (2011), doi:10.1016/j.coastaleng.2011.04.003

parameter is to widen the range of particle sizes over which deposition may occur relative to Fig. 6, and permit wider possibilities for simultaneous erosion and deposition.

Visual inspection of Fig. 6 may suggest that there would always be more deposition in PR than in MVR. That this is not so can be understood by increasing the variability of the parameters to, say, ±3 standard deviations (i.e. 99.8% of the total probability). This would mean that the zone of overlap between erosion and deposition would cover a much wider range of particle sizes than for ±1 standard deviations. In that circumstance, over time erosion classes, although not necessarily the total erosion flux, will dominate deposition classes when aggregation is accounted for. In other words the effects of probabilistic treatment would be more pronounced for erosion than for deposition. This difference occurs because erosion, involving interactions among the pdfs of bed shear strength and shear strength, amounts to an amplification of the probabilistic effect. In contrast, deposition is controlled by the settling velocity spectrum along with the probability of re-entrainment of the material approaching the bed. However, re-entrainment is essentially erosion, which is therefore reinforced.

The range of particle sizes that can experience simultaneous erosion and deposition as a result of probabilistic representation is shown in Fig. 8 based on ±1 standard deviations. This particle size range of simultaneous erosion and deposition would be much broader for the "full" (i.e. 99.8% of probability) pdf of each variable.

6. Modes of exchange

The above analysis identifies four modes in which bed exchange can be modeled. The first two rely on mean-value representations of the governing variables. They are: (1) Modeling bed exchange in accordance with Fig. 5 denoted as exclusive mean-value representation (EMVR). (2) With EMVR modified by suppressing the role of the critical shear stress for deposition we have simultaneous mean-value representation (SMVR), which permits continuous deposition. The simultaneous modes allow for continuous deposition at all shear stress conditions as proposed by Sanford and Halka (1993), whereas the exclusive modes permit deposition only when the shear stress is below the critical deposition threshold.

The remaining two modes are based on probabilistic representations: (3) the protocol in Figs. 7 and 8, a probabilistic extension of Fig. 5, is exclusive probabilistic representation (EPR). (4) A probabilistic extension of SMVR is simultaneous probabilistic representation (SPR).

For an assessment of the significance of these bed exchange modes the following steps were carried out:

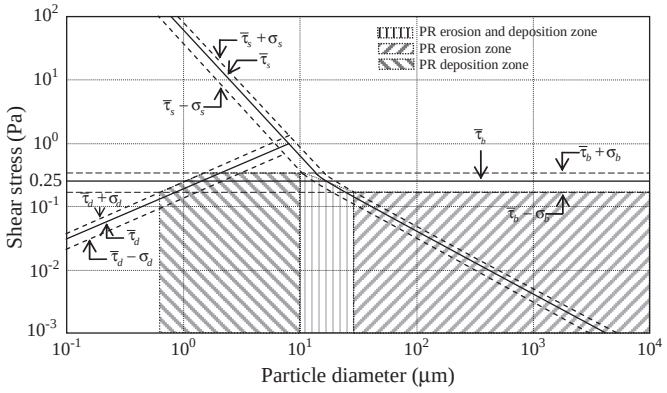

Fig. 8. Zone of simultaneous erosion and deposition associated with the probabilistic representation of Fig. 7.

(1) The four modes were incorporated into a numerical code for calculating the instantaneous suspended sediment concentration in the three dimensional space, although applications to CRAF data were limited to vertical transport. The suspended sediment concentration was obtained as the sum of the concentrations determined by solving the mass balance equation for each size class within the selected particle size range. The sediment was divided into 60 classes between 0.1 μm and 2000 μm. In preliminary simulations, the instantaneous concentration profile in laboratory setting was found to be reasonably represented by five vertical grid cells in the model. All four bed exchange modes used the full particle size distribution.

(2) For calculations of the shear stress and the flow shear rate required for settling velocity estimation at any elevation in the water column, logarithmic distribution of the horizontal velocity and the Darcy–Weisbach friction factor (=0.020) reported by Mehta (1973) in reference to the CRAF were selected. Vertical diffusion was calculated initially by employing the *k*-epsilon scheme for turbulence closure following Hsu et al. (2007). It was later found that eddy diffusivity based closure was an adequate substitute for accuracy and substantially reduced the computation time. The diffusion coefficient was derived from measurements by Mehta (1973) in the CRAF. All four modes used this approach.

(3) An algorithm was included for aggregation kinetics permitting sediment mass exchange between classes due to floc growth and breakup. For that purpose the multi-class modeling framework outlined by McAnally and Mehta (2001, 2002) and provided in detail by McAnally (1999) was used. The basis of aggregation kinetics is that the frequency of collision is a function of the number concentration of suspended particles and forces that tend to bring the particles close enough to collide. Once collision occurs the efficiency of coherence, which is the probability that the particles will form a larger floc, is invoked. An efficiency coefficient is also assigned for disaggregation, whereby collisions cause flocs to break apart into smaller units. Disaggregation is considered to be due to flow shear. All four modes included the flocculation model (aggregation and disaggregation).

(4) In regard to the bed shear stress, Christensen (1965) pointed out that the experimental data on the fluctuating bed shear stress used by Einstein (1950) could be appropriately modeled as a non-normal pdf. Winterwerp and van Kesteren (2004) underscored the significance of skewness in the pdf as representing large bursting events which promote more erosion relative to normally distributed pdf. For three sets of experimental data of Krone (1962) on the transport of mud from the San Francisco Bay, Winterwerp and van Kesteren used an analytical expression for the bed shear stress pdf in which the standard deviation varied from test to test. In the present study the bed shear pdf was developed from the pdf of the horizontal velocity assumed to be a random variable and conveniently relying on the quadratic relationship between the bed shear stress and velocity in turbulent flows. Given this relationship, Monte Carlo simulation was performed using the cumulative density function of velocity ranging from a minimum value with a probability of 0 to a maximum with a probability of 1. For validation of the approach the standard deviation of the velocity pdf was adjusted to reproduce the bed shear stress pdfs of Winterwerp and van Kesteren, each time using 10^7 random velocity values and 200 partitions of both velocity and shear stress. The critical shear stress for deposition and the bed shear strength were considered to follow normal distribution found to be reasonable for the experiments of Self et al. (1989). All distributions used numerical integration based

Please cite this article as: Letter, J.V., Mehta, A.J., A heuristic examination of cohesive sediment bed exchange in turbulent flows, Coast. Eng. (2011), doi:10.1016/j.coastaleng.2011.04.003

on a discretization of the pdfs with 101 discrete values, and truncation of the tails of the distributions at ±3 three standard deviations relative to the mean representing about 99.8% of the total probability. Only the SPR and EPR modes used the shear stress distribution.

(5) For calculation of the deposition flux the settling velocity was treated as a probabilistic variable and calculated from the expression of Teeter (2001) in which the effects of local concentration and flow shear rate are accounted for. For that calculation the pdfs of the local shear stress in the water column and from it the flow shear rate were assumed to be proportional to the pdf of the bed shear stress, since each of these variables is derived from their quadratic dependence on the flow velocity. The maximum settling velocity was set at 2×10^{-4} m s^{-1} as deduced by Mehta and Lott (1987). Only the SPR and EPR modes used the probabilistic treatment. All modes had the maximum settling velocity imposed. The classical critical shear stress for deposition was applied in the EPR and EMVR modes. The threshold for EMVR was a single value for each size class. For EPR the threshold was probabilistic and the deposition flux was the result of integration of the threshold function using the probability distributions of the shear stress and the shear strength. For the SMVR and SPR modes deposition was computed for each class without a threshold applied.

(6) The erosion flux was modeled within the framework described by van Prooijen and Winterwerp (2010). This is a revision of the equation of Partheniades (1965) relating the erosion flux to the time-mean bed shear stress within the definition of the probability of erosion defined by Einstein (1950). A critically limiting feature of the Partheniades equation arises from the assumption that the characteristic time inherent to the chosen mechanism for particle detachment from the bed is independent of the flow condition, when in fact this time must decrease as the bed shear stress increases. The outcome is that the original equation predicts a maximum erosion rate that cannot be exceeded irrespective of the value of the bed shear stress. This error is corrected for in the revised equation by redefining the characteristic time and the function involving the probability of erosion. The revised equation for the erosion flux ε_i for a specific particle size is

$$\varepsilon_i = \frac{C_b f_i}{\sqrt{\rho_w}}\left[\begin{array}{l}\int_0^{\infty}\int_0^{\infty}\tau_b^{1/2} f(\tau_b)H(\tau_b-\tau_s)d\tau_s\,d\tau_b + \\ + \int_{-\infty}^{0}\int_{-\infty}^{0}\tau_b^{1/2} f(\tau_b)[1-H(\tau_b-\tau_s)]d\tau_s\,d\tau_b\end{array}\right] \quad (3)$$

where C_b is a representative bottom bed concentration, f_i the fraction of the size class in the bed, f the frequency distribution and H the Heaviside function. Whereas van Prooijen and Winterwerp made assumptions that allowed for an analytical solution of Eq. (3), in the current model the integration was performed numerically (Letter 2009). Eq. (3) was shown to satisfactorily simulate CRAF erosion test results of Parchure (1984) using kaolinite in saltwater. Eq. (3) was used only in the SPR and EPR modes. The mean-valued modes used the classical excess shear stress method.

(7) Using calculated values of erosion and deposition fluxes, bed exchange was achieved by numerical integration of the appropriate products of the pdfs of the variables and their interactions within the framework of particle aggregation kinetics. A requirement for modeling is setting, at the bed surface, the initial unit sediment concentration, i.e. sediment dry mass per unit bed volume and unit bed depth. The distribution of the unit concentration as a function of sediment class was based on guidance from the primary particle size distribution of kaolinite, its flocculation behavior in saltwater and trial simulations of floc size distributions based on aggregation kinetics. It was found that the model results were only weakly sensitive to the initial specification of the unit concentration by class. All modes used the same bed initialization of size class distribution.

Based on the results of numerical modeling described elsewhere (Letter 2009), we will illustrate the effects of probabilistic versus mean-value representations of variables by making use of the deposition test runs of Fig. 2 and the dilution test data in Fig. 3.

7. Significance of probabilistic representation

7.1. Deposition runs

The model was used to solve for the time-variation of the depth-mean suspended sediment concentration for conditions relevant to the data in Fig. 2 and experimental coefficients given in Table 1 with some adjustments to calibrate the model to the SMVR mode of bed exchange. The calibrated values remained unchanged in simulations for all the modes. The distribution of the initial unit concentration at the bed surface was limited to the first 40 size classes, decreasing from 0.0325 kg m^{-2} at 0.1 μm to 0.02 kg m^{-2} at 70 μm, the upper value of the primary particle diameter. For all higher size classes the initial unit concentration was taken as zero.

Values of the efficiencies of coherence and disaggregation kinetics were based on estimates provided by McAnally (1999). Aggregation was permitted for concentrations lower than 0.66 kg m^{-3} taken as the limit above which incipient effects of hindered settling were found to limit the efficacy of aggregation.

For an assessment of probabilistic representation, in Fig. 9 the four deposition runs are compared with simulations based on SMVR. In each case the concentration reaches its expected residual value, although for the middle two runs the approach to residual concentration deviates from measurement especially in the first hour. The residual concentration is the outcome of equilibrium between the total erosion and deposition fluxes, with contributions from classes represented in the system. Simulations for the two middle bed shear stress runs indicate higher than measured concentrations, because the number of degrees of freedom in model specification made precise agreement difficult to achieve. For the run at the lowest bed shear stress (0.25 Pa) with the highest rate of deposition, switching from SMVR simulation to EMVR substantially increases the residual concentration; at 6 h the EMVR value (0.4 kg m^{-3}) is more than double the SMVR value. As a consequence of deposition over the entire range of suspended particle size in SMVR, as opposed to restricted deposition introduced by the critical shear stress for deposition in EMVR, SMVR results in lower residual concentration.

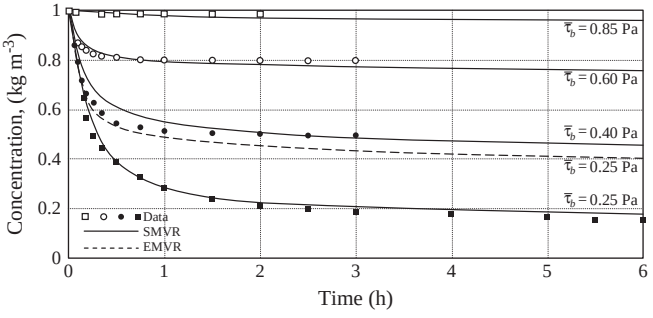

Fig. 9. Time-variation of concentration (data points) of kaolinite in CRAF deposition tests in Fig. 2 and mean-value simulations without (EMVR) and with (SMVR) continuous deposition.

Please cite this article as: Letter, J.V., Mehta, A.J., A heuristic examination of cohesive sediment bed exchange in turbulent flows, Coast. Eng. (2011), doi:10.1016/j.coastaleng.2011.04.003

The significance of incorporating probabilistic representation is further illustrated in Fig. 10 for the 0.40 Pa shear stress run. At this comparatively high shear stress the effect of exchange mode on concentration variation can be expected to be high. Comparison of EMVR simulation with EPR shows that increased variability introduced by the probabilistic treatment leads to a higher residual concentration due to increased erosion in EPR. Simultaneous deposition causes the residual concentration to be lower (as in the 0.25 Pa run, Fig. 9) for both the mean-value (SMVR) and the probabilistic (SPR) approaches. Deviations between the outputs and data in all four cases are artifacts of the use of a single set of parameters (including those in Table 1) for all simulations. If calibration were to be performed using either EMVR or SMVR to replicate the results for EPR or SPR, a revised set of the coefficients would be required.

7.2. Dilution test

Referring to the data in Fig. 3 during the fluid extraction phase, the reduction in depth-averaged concentration C due to pure dilution, i.e. absence of bed exchange, would be given by

$$\frac{C}{C_0} = e^{-\frac{q}{h}t} \tag{4}$$

where $C_0 = 3.85$ kg m^{-3} is the initial concentration, $h = 0.26$ m is the water depth and $q = 8.77 \times 10^{-5}$ m^3 s^{-1} m^2 is the prescribed extraction rate. It is assumed that the effects of extraction on concentration are vertically uniform within the CRAF, while recognizing that longitudinal uniformity is assured in that apparatus.

In Fig. 11, Eq. (4) is observed to match the data well confirming that during the extraction procedure erosion was negligible. The numerical model, applied under the same conditions of extraction without bed exchange, very closely matches the equation and the data. This numerical test was performed to validate the extraction specification in the model.

The model was then set up with bed exchange switched on. In this case the initial suspended sediment concentration was set to zero, the initial bed surface (unit) concentration was taken as 0.046 kg m^{-2} below 70 μm and zero above. The total bed mass was adjusted until, due to erosion during the initial spin-up of the model, the concentration in suspension approached the equilibrium value of 3.85 kg m^{-3}. The model was run for 5 days, having reached near-equilibrium in about an hour, and then fluid extraction begun at hour 120 and continued until hour 124. Model simulation was further continued for 24 h (hour 148).

In Fig. 12, EMVR, SMVR, EPR and SPR simulations have been compared with data from Fig. 3. Starting from the inception of the test, the simulations approached 3.85 kg m^{-3} within the same time frame and are represented by a single curve, except for the SPR curve which overshot the 3.85 to an equilibrium at 4.30 kg m^{-3}. During the first 2 h of extraction the simulations closely follow the data. During the remaining 2 h, EMVR and SMVR continue to mimic Eq. (4) for pure dilution, and after the cessation of extraction both remain constant at the final concentration of 0.030 kg m^{-3} for the EMVR and 0.036 kg m^{-3} for the SMVR. In contrast, EPR and SPR both generate a small erosion flux reflected by the slight positive deviation of the (dashed) curve from Eq. (4). More importantly, EPR and SPR both indicate erosion after dilution, increasing the concentration to 0.1 kg m^{-3} at hour 148 in agreement with the data. Although the erosion flux between hours 124 and 148 is low compared to the erosion flux at the inception of the test, it underscores the importance of both multi-class representation of particle size and the probabilistic treatment of erosion-governing variables (bed shear stress and shear strength). The EPR and SPR trends after hour 128 indicate that deposition was not significant in the SPR simulation during that period.

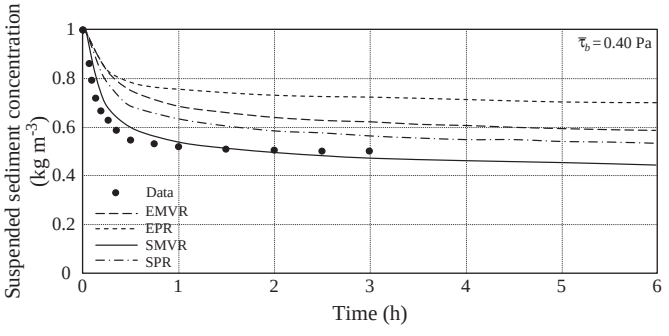

Fig. 10. Comparison between deposition data from Fig. 2 at 0.40 Pa shear stress and simulations based on EMVR, SMVR, EPR and SPR.

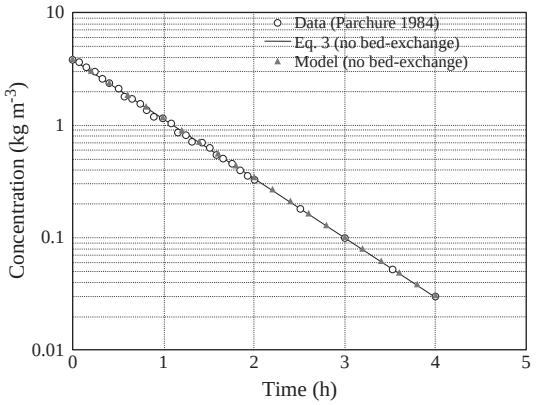

Fig. 11. Comparison of dilution test data for kaolinite in the CRAF with Eq. (4) (pure dilution) and numerical model result (without bed exchange).

7.3. Particle size distribution

Lau and Krishnappan (1994) carried out deposition tests on kaolinite in an annular flume larger than the CRAF with a mean diameter of 5 m. Mean trends in their tests were similar to those shown in Fig. 2. By periodically monitoring the suspended floc size distribution it was shown that the distribution changed as the concentration decreased and eventually approached a residual value. The change in distribution during deposition showed reductions in concentration of all classes, but with greater reductions in the larger flocs. This observation was supportive of the earlier inference by Lick (1982) indicating that, in general, both multi-size class effect and aggregation result in a shift in the size spectrum with time until a residual concentration is reached.

In the CRAF experiments the initial, dispersed particle distribution of kaolinite was known. Based on the quiescent settling data obtained Yeh (1979) for the same sediment, Mehta and Lott (1987) deduced an approximate distribution of the settling velocity of kaolinite applicable to the CRAF tests, in which the flow was turbulent. Partly based on the corresponding floc size distribution, Letter (2009) assigned particle size classes (and initial unit class concentrations) in the present study.

Numerically generated results from the dilution test are presented in Fig. 13 in terms of the dependence of the volume concentration C_v (volume of dry particles divided by volume of suspension) on particle size. Simulations used the same kaolinite properties, critical shear stress for deposition and shear strength. Comparison between SMVR and SPR simulations at the initiation of dilution at hour 120 shows sharply different distributions. SPR results in significantly larger flocs with a modal diameter of about 300 μm, compared to about 70 μm in SMVR. The modal diameter at the end of dilution (hour 124) dropped dramatically in both the mean and probabilistic treatments, with the

Please cite this article as: Letter, J.V., Mehta, A.J., A heuristic examination of cohesive sediment bed exchange in turbulent flows, Coast. Eng. (2011), doi:10.1016/j.coastaleng.2011.04.003

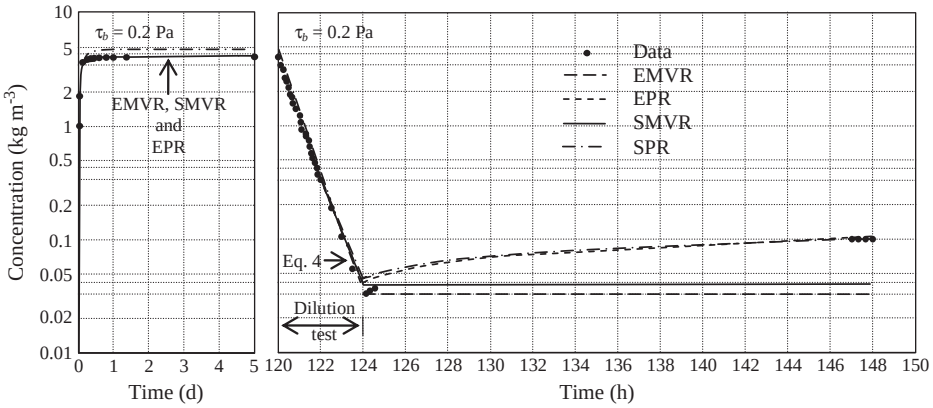

Fig. 12. Test data of Fig. 3 compared with EMVR, SMVR, EPR, SPR and Eq. (4) (during dilution).

SPR modal size of 15 μm only slightly smaller than 18 μm in SMVR. These low values and their closeness indicate the controlling role of extraction on particle size during the 4-hour period. After dilution SPR retained its broader spectral character compared to SMVR. In the latter mode, the distribution at the end of the simulation at hour 138 had not changed much from the output at hour 124. In contrast, the SPR distribution shows an extension into larger floc sizes, which is qualitatively consistent with the observations of Kranck and Milligan (1992) based on their size distribution measurements of sediment from the San Francisco Bay. The probabilistic variables result in a greater collision frequency compared to the mean-value representation, which in turn increases the inter-particle mass-class fluxes. As a result, sediment transport occurs over a wider range of sizes during bed exchange and leads to a broader spectrum as flocs grow.

Figs. 14 through 16 show the effects of the mode of bed exchange on the particle size distribution at hours 120, 124 and 138. The probabilistic modes (SPR and EPR) have broader range of particle sizes than the mean-value modes (EMVR and SMVR). At hour 120, EMVR and SMVR are almost indistinguishable, both peaking at 70 μm. SPR and EPR are very similar at hour 120 with SPR having a slightly higher modal concentration at a slightly smaller floc size (266 μm for SPR versus 315 μm for EPR). SPR has a slightly higher concentration distribution than EPR at hours 124 and 138, mainly because of greater erosion prior to dilution. At hour 138 both SPR and EPR show expansion of the floc size distribution on the high-side of the distribution, with the low-side remaining the same compared to the end of dilution at hour 124. The differences between the mean-value and the probabilistic modes are much larger than the differences between exclusive (EMVR and EPR) and simultaneous modes (SMVR and SPR).

8. Concluding comments

The main points to be made are that interpretation of the CRAF data on suspended sediment concentration changes with time using kaolinite can be significantly facilitated when: (1) particle size is treated as a multi-class representation, (2) the kinetics of aggregation describing collisional growth and breakup of suspended particles is accounted for and, (3) the bed shear stress, the critical shear stress for deposition and the floc shear strength are treated as probabilistic variables specified by their pdfs.

A basic feature of the analysis is the description of the variation with size of the critical shear stress for deposition given by Eq. (1) and the shear strength by Eq. (2). These two equations are combined and interpreted in terms of the zones of bed exchange in Fig. 4. A probabilistic interpretation of the variables associated with this description combined with aggregation of eroding and depositing particles is modeled to produce the observed time-variation of suspended sediment concentration.

In general, a decrease or increase in concentration with time, or attainment of a constant value, is the result of a combination of erosion and deposition fluxes over a range of particle sizes. In this a significant effect of aggregation is that it brings about time-dependent shifts in suspended particle size distribution; erosion and deposition

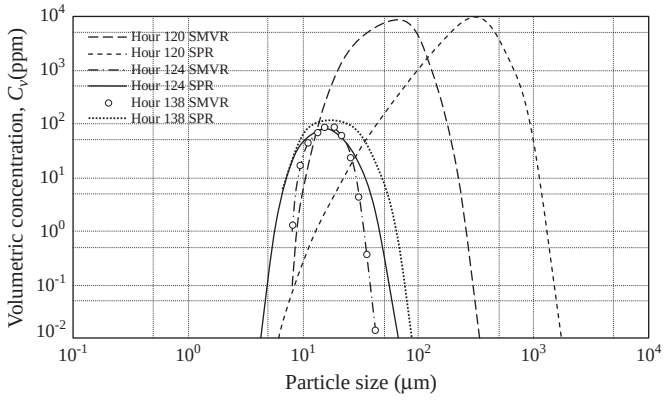

Fig. 13. Simulated particle size distributions for mean-value and probabilistic representations of the dilution test of Fig. 3.

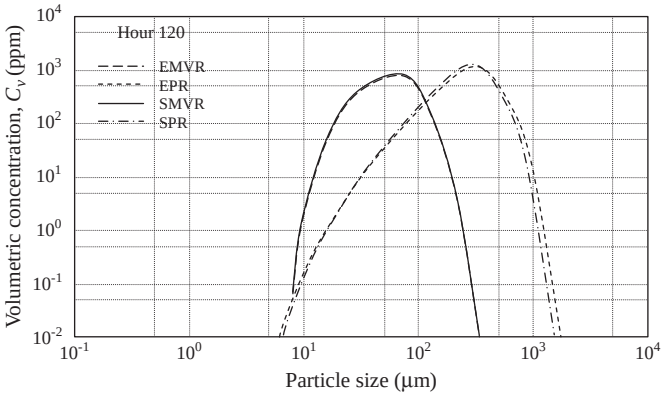

Fig. 14. Comparison of bed exchange mode on particle size distribution at hour 120 after initial erosion.

Please cite this article as: Letter, J.V., Mehta, A.J., A heuristic examination of cohesive sediment bed exchange in turbulent flows, Coast. Eng. (2011), doi:10.1016/j.coastaleng.2011.04.003

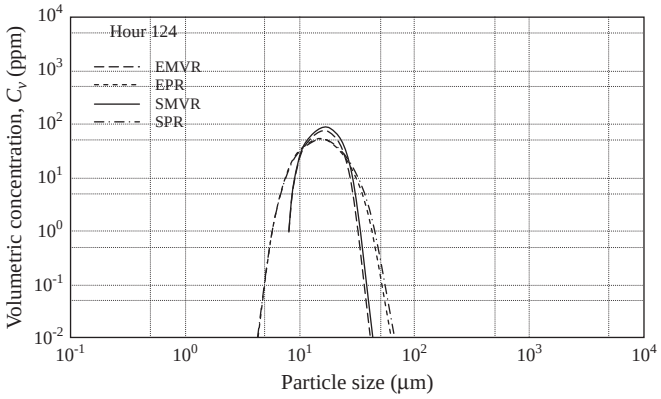

Fig. 15. Comparison of bed exchange mode on particle size distribution at hour 124 after dilution.

fluxes are accordingly modulated and they in turn influence the rate of change of concentration. The role of probabilistic treatment is to broaden the spectrum (relative to mean-value representation) due to increased possibilities of inter-particle interactions, which result in the formation of larger flocs.

The mode of bed treatment used within any numerical model requires calibration to the sediments being simulated. There is no general guidance yet developed for which treatment may perform most effectively. However, care must be taken if a simplified mode is chosen and the range of calibration conditions is significantly changed during any prognostic phase of the study that affects the basic distributions of the primary variables.

Simple models of erosion and deposition that rely on the single-size assumption and mean-value representation of variables do not resolve the mechanistic basis underpinning the dynamics of suspended sediment concentration. The reliability of such models is largely based on empirical calibration, which in the strict sense precludes their use for prediction purposes. The conventional distinction between exclusive and simultaneous modes of transport loses meaning when the multi-class probabilistic analysis is adopted.

Further exploration of Eqs. (1) and (2) is important for confirmation of the inferences drawn. The versatility of these expressions for application purposes is presently quite limited. For example, since floc size depends on the suspended sediment concentration and the flow shear rate, the exponent ξ must be treated as a variable related to these two factors, which in turn could have a significant effect on the shape of the curve relating the critical shear stress to diameter. As for Eq. (2), its rheological basis remains to be verified with use of advanced rheometry not available for mud studies when the original viscometer tests were carried out. The consistency of Eqs. (1) and (2) in practical applications can be achieved to some extent indirectly by comparing the simulated size spectra with measured ones, which was not attempted in this cursory investigation. The experimental data of Lau and Krishnappan (1994) are a likely choice for further analysis.

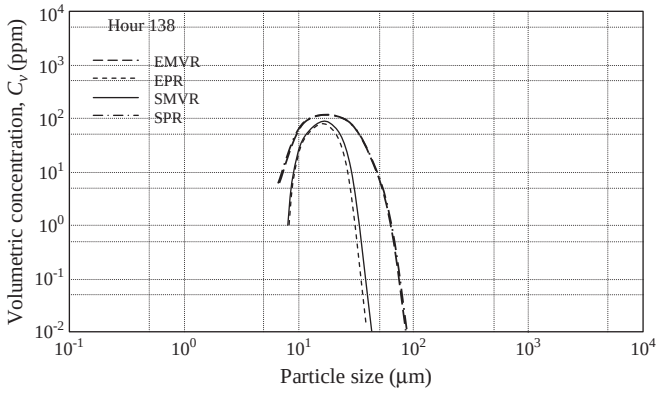

Fig. 16. Comparison of bed exchange mode on particle size distribution at hour 138 4-hour after end of dilution.

Acknowledgments

The first author was financially supported during the study by the U.S. Army Engineer Research and Development Center (ERDC). The second author received funding from the Office of Naval Research project no. N00014-07-1-0448.

References

Bagnold, R.A., 1966. An approach to the sediment transport problem from general physics. Professional Paper No. 442-I. U.S. Geological Survey, Washington, DC.
Christensen, B.A., 1965. Discussion of "Erosion and deposition of cohesive soils", by E. Partheniades. J. Hydraul. Div., ASCE 91 (5), 301–308.
Einstein, H.A., 1950. The bed-load function for sediment transportation in open channel flows. Technical Bulletin No. 1026. U. S. Department of Agriculture, Washington, DC.
Hsu, T.-J., Traykovski, P.A., Kineke, G.C., 2007. On modeling boundary layer and gravity-driven fluid mud transport. J. Geophys. Res. 112 (C04011). doi:10.1029/ 2006J C003719.
Khelifa, A., Hill, P.S., 2006. Models for effective density and settling velocity of flocs. J. Hydraul. Res. 44 (3), 390–401.
Kranck, K., Milligan, T.G., 1992. Characteristics of suspended particles at an 11-hour anchor station in San Francisco Bay, California. J. Geophys. Res. C7, 11,373–11,382.
Kranenburg, C., 1994. The fractal structure of cohesive sediment aggregates. Estuarine Coastal Shelf Sci. 39 (5), 451–460.
Krone, R.B., 1962. Flume studies of the transport of sediment in estuarial shoaling processes. Final Report. Hydraulic Engineering Laboratory and Sanitary Engineering Research Laboratory, University of California, Berkeley.
Krone, R.B., 1963. A study of rheological properties of estuarial sediments. Technical Bulletin No. 7, Committee on Tidal Hydraulics. U.S. Army Engineer Waterways Experiment Station, Vicksburg, MS.
Lau, Y.L., Krishnappan, B.G., 1994. Does reentrainment occur during cohesive sediment settling? J. Hydraul. Eng. 120 (2), 236–244.
Letter, J.V., 2009. Significance of probabilistic parameterization in cohesive sediment bed exchange. PhD thesis, University of Florida, Gainesville.
Lick, W., 1982. Entrainment, deposition and transport of fine-grained sediment in lakes. Hydrobiologia 91 (2), 31–40.
Mantz, P.A., 1977. Incipient transport of fine grains and flakes by fluids—extended Shields diagram. J. Hydraul. Div., ASCE 103 (6), 601–615.
McAnally, W.H., 1999. Transport of fine sediments in estuarial waters. PhD thesis, University of Florida, Gainesville.
McAnally, W.H., Mehta, A.J., 2001. Collisional aggregation of estuarial fine sediment. In: McAnally, W.H., Mehta, A.J. (Eds.), Coastal and Estuarine Fine Sediment Processes. Elsevier, pp. 19–39.
McAnally, W.H., Mehta, A.J., 2002. Significance of aggregation of fine sediment particles in their deposition. Estuarine Coastal Shelf Sci. 54, 643–653.
Mehta, A.J., 1973. Depositional behavior of cohesive sediments. PhD thesis, University of Florida, Gainesville.
Mehta, A.J., Lee, S.-C., 1994. Problems in linking the threshold condition for the transport of cohesionless and cohesive sediment grains. J. Coastal Res. 10 (1), 170–177.
Mehta, A.J., Lott, J.W., 1987. Sorting of fine sediment during deposition. In: Kraus, N.C. (Ed.), Proceedings of Coastal Sediments'87. ASCE, New York, pp. 348–362.
Mehta, A.J., Partheniades, E., 1975. An investigation of the depositional properties of flocculated fine sediments. J. Hydraul. Res. 4, 361–381.
Migniot, P.C., 1968. A study of the physical properties of different very fine sediments and their behavior under hydrodynamic action. Houille Blanche 7, 591–620 (in French, with abstract in English).
Parchure, T.M., 1984. Erosional behavior of deposited cohesive sediments. PhD thesis, University of Florida, Gainesville.
Parchure, T.M., Mehta, A.J., 1985. Erosion of soft cohesive sediment deposits. J. Hydraul. Eng. 111 (10), 1308–1326.
Partheniades, E., 1965. Erosion and deposition of cohesive soils. J. Hydraul. Div., ASCE 91 (1), 105–138.
Sanford, L.P., Halka, J.P., 1993. Assessing the paradigm of mutually exclusive erosion and deposition of mud, with examples from upper Chesapeake Bay. Mar. Geol. 114 (1–2), 35–37.
Self, R.F.L., Nowell, A.R.M., Jumars, P.A., 1989. Factors controlling critical shears for deposition and erosion of individual grains. Mar. Geol. 86, 181–199.
Teeter, A.M., 2001. Clay–silt sediment modeling using multiple grain classes, part I: settling and deposition. In: McAnally, W.H., Mehta, A.J. (Eds.), Coastal and Estuarine Fine Sediment Processes. Elsevier, pp. 157–171.

Please cite this article as: Letter, J.V., Mehta, A.J., A heuristic examination of cohesive sediment bed exchange in turbulent flows, Coast. Eng. (2011), doi:10.1016/j.coastaleng.2011.04.003

Tolhurst, T.J., Black, K.S., Paterson, D.M., 2009. Muddy sediment erosion: insights from field studies. J. Hydraul. Eng. 135, 73–87.
van Prooijen, B.C., Winterwerp, J.C., 2010. A stochastic formulation for erosion of cohesive sediments. J. Geophys. Res. 115, C01005. doi:10.1029/2008JC005189.
Winterwerp, J.C., 1998. A simple model for turbulence induced flocculation of cohesive sediment. J. Hydraul. Res. 36 (3), 309–326.
Winterwerp, J.C., van Kesteren, W.G.M., 2004. Introduction to the Physics of Cohesive Sediment in the Marine Environment. Elsevier.
Wolanski, E., 2007. Estuarine Ecohydrology. Elsevier.
Yeh, H.Y., 1979. Resuspension properties of flow deposited cohesive sediment beds. MS thesis, University of Florida, Gainesville.

Please cite this article as: Letter, J.V., Mehta, A.J., A heuristic examination of cohesive sediment bed exchange in turbulent flows, Coast. Eng. (2011), doi:10.1016/j.coastaleng.2011.04.003